Sensing and Bio-Sensing Research 3 (2015) 53–58

Contents lists available at ScienceDirect

Sensing and Bio-Sensing Research

journal homepage: www.elsevier.com/locate/sbsr

On-chip detection performed by amorphous silicon balanced photosensor for lab-on chip application

G. de Cesare [a,*], A. Nascetti [b], R. Scipinotti [a], A. Zahra [c], D. Caputo [a]

[a] Department of Information, Electronic and Telecommunication Engineering, Sapienza University of Rome, Italy
[b] Department of Astronautics, Electrical and Energy Engineering, Sapienza University of Rome, Italy
[c] Center for Life Nano Science@Sapienza, Istituto Italiano di Tecnologia, Sapienza University of Rome, Italy

ARTICLE INFO

Keywords:
Balanced photodiode
Differential measurement
Amorphous silicon
Photosensor
Microfluidic
Lab-on-chip

ABSTRACT

In this paper we have integrated a two-channel microfluidic network, fabricated by molding two polydimethilsiloxane channels, with a balanced photodiode constituted by two series-connected amorphous silicon/silicon carbide n-i-p stacked junctions, deposited by Plasma Enhanced Chemical Vapor Deposition on a glass substrate. The structure takes advantage of the differential current measurement to reveal very small variations of photocurrent in a large background current signal suitable for biomedical application. The microfluidic network has been fabricated with dimensions of 3 cm × 2 mm × 150 μm ($L \times W \times H$) for each channel.

The experiments have been carried out measuring the differential current in several conditions. All the experiments have been executed under a large background light intensity to reproduce realistic operating conditions in biomedical applications. We have found that the proposed device is able to detect the presence or absence of water flow in the channel and the presence of fluorescent marker. In particular, under identical channel conditions the differential current is at least a factor 60 lower that the current flowing in each diode.

1. Introduction

During the last years lab-on-chip (LOC) systems have shown their relevance as a powerful instrument for complex chemical or bio-chemical analysis [25]. The concept of the micro Total Analysis Systems (μTAS) and the development of MEMs technologies led to the development of LoC systems as a powerful tool in point-of-care applications. In particular, several steps of analysis (sample preparation, mixing, movement and detection) are integrated on a single device with different functional modules [15,28]. These analyses are commonly performed using spectroscopic and chromatographic properties or the survey of bio-luminescence and chemiluminescence characteristics [14] of the sample. The advent of miniaturized array technology has enabled parallel and multiple comparative measurements of different samples combining together high sensitivity, low sample consumption, high-throughput and rapidity of the analysis [21,24]. However, even though the successful miniaturization of the analytical format is obtained by microfluidic structures, this is not flanked by an adequate miniaturization of the detection technique [18,1], which, in most cases, is done off-chip. On-chip detection is still therefore a challenge for improving sensitivity and compactness [26,19,35].

Recently different groups, including ours, have integrated electrical and/or optical sensors with the microfluidics leading to LOC systems to reduce the external instrumentation needed to perform the analysis task [2,3,22,27,31,30,29]. In particular optical detection of biomolecules based on the use of thin film photosensors have been developed. Two main categories have been explored: the first based on the detection of the light intensity emitted by fluorescent markers attached to the molecules (labeled detection) [20,4]), the second based on the measurements of the molecules optical absorbance in specific wavelength range (label free detection) [17].

One of the most promising materials to this aim is hydrogenated amorphous silicon (a-Si:H) and its alloy [33]. The low deposition temperature (below 250 °C) and its physical characteristics prompt the use of this material in different device such as solar cells [13], electronic switching [5], strain sensors [16] and photosensors [6]. The use of thin film a-Si:H photosensors for the detection of biomolecules has been already developed by the authors in both labeled and label free techniques. In particular: the authors propose detection systems: for Ocratoxin A in wine, based on the coupling of a Thin Layer Chromatography plate with an array of

* Corresponding author.

http://dx.doi.org/10.1016/j.sbsr.2014.12.005
2214-1804/

amorphous silicon photodiodes [7]b; [8], for DNA labeled with Alexa Fluor 350 [9], and for an on-chip DNA label free detection system, based on the measurements of different absorbance in the UV range, of single and double stranded DNA molecules system [17].

In all these experiments current variations in the order of pico-amps had to be resolved from the several tens of nanoamps background current. In this case a trade-off between dynamic range and resolution has to be considered: indeed, the large photocurrent due to the large background radiation reduces the voltage swing at the amplifier output if high gain (for the transimpedance amplifier) or a high integration time (for the charge sensitive amplifier) are used. On the other hand a low gain or a low integration time, reduces the sensitivity of the system.

In electronic circuits a common way to eliminate background signal consists in using differential readout approaches [23]. Balanced structures are extensively used to reject large common signals and to amplify only their difference.

The authors have presented a balanced photodiode based on amorphous silicon (a-Si:H)/amorphous silicon carbide (a-SiC:H) thin film photosensors [10,11], whose spectral response extends down to the ultraviolet range. The structure is a single detector, that, combining two sensors, gives, in a hardware way, as output signal directly the differential current. This permits a high dynamic range in the signal measurement without degrading the resolution of the single photosensor and gives the possibility to reveal very small variations of photocurrent in a large background current signal.

In this paper we present the integration of the balanced photosensor with a microfluidic network to perform high-dynamic, high-sensitive on-chip detection. This kind of integration is a challenging issue in the scientific community working on lab-on-chip systems for biomedical applications [32]. The paper is organized as follows: in Section 2 the structure and the operation mode of the integrated system are described; in Section 3 the fabrication process and the characterization of the sensor structure is reported together with the fabrication process of the microfluidic network and their integration; in Section 4 experimental results, carried out measuring the differential current of the balanced structure in several conditions, are described in details and discussed.

2. Structure and operation of the device

The device combines on the same side of a glass substrate a differential photodiode aligned with two microfluidic channels. Fig. 1 reports its cross section and top view. From the cross section, we see that the single sensor of the balanced device is a n-doped/intrinsic/p-doped a-Si:H stacked structure and that the balanced device is achieved connecting in series two a-Si:H/a-SiC:H n-i-p sensors. A polymer film (SU-8) acts as insulating and passivation layer. The two microchannels are made in polydimethilsiloxane and are placed on top of the passivation layer. The inner walls of the microchannels have been properly treated to make them hydrophilic.

Assuming photosensors perfectly matched and uniform light radiation distribution, differences in luminescence or absorption phenomena occurring inside the two channels produce differences in the light impinging on the two photosensors of the balanced device and give rise to a differential current flowing through the common electrode. It is worth noticing that, integrating the balanced photodiode and the microfluidic network on the same side of the glass substrate, the distance between the photosensors and the microfluidic channels is reduced to the few microns of the SU-8 thickness. This implies a maximization of the light impinging on the photosensors and a reduction of the inter-channel crosstalk. Furthermore, the n-i-p structure used in this work results in a device with very low dark current, that is useful to maximize the signal-to-noise ratio. Indeed in this structure, the deposition temperature of the three subsequent layers decreases through the whole process, thus reducing doping contamination of the i-layer, which would have lead to the increase of the dark current due to thermal carrier generation [34].

The corresponding electronic circuit and the read-out electronics are depicted in Fig. 2, where the differential readout approach eliminates the background signal. Indeed, thanks to the virtual ground of the operational amplifier, the two diodes are biased at the same reverse voltage, therefore if the two diodes are perfectly matched the output voltage of the amplifier is proportional only to the difference between the currents flowing through the two photosensors, which in turn is related to the difference between the light intensities impinging on the sensors.

In addition, the differential approach reduces the effect of the common mode signal due to temperature variations and/or instability of light source.

3. Fabrication and characterization of the device

The device fabrication is mainly devoted to the balanced photodiode, because the network microfluidic requires few technological steps as well as its assembling with the differential structure.

3.1. Balanced photodiode

The structure of each sensor is constituted by an amorphous silicon/amorphous silicon carbide heterojunction, deposited on a glass substrate covered by a thin metal film electrode (bottom electrode). The top sensor electrode is a two-layer structure constituted by an ultra thin chromium silicide (CrSi) layer formed on top of the p-doped layer [12] and by a thin film metal grid that allows the transmission of the incident radiation into the active layer of the device. A network of metal lines, deposited on an insulating layer allows the series configuration of the two diodes and the

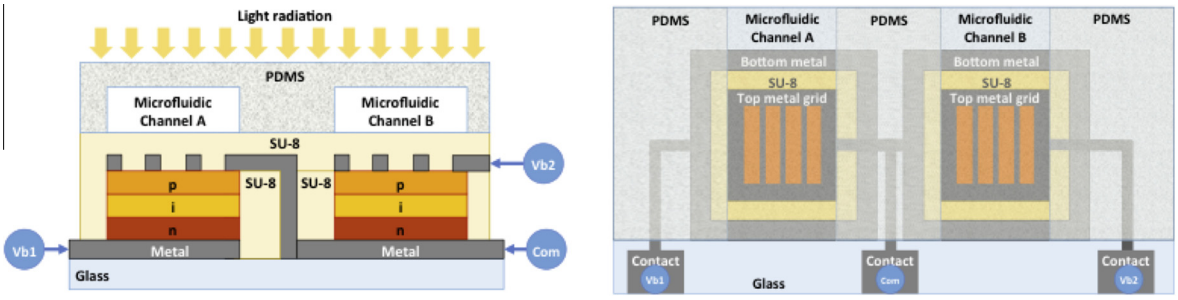

Fig. 1. Cross section (right) and top view (left) of the amorphous silicon balanced photosensor integrated with two PDMS microfluidic channels.

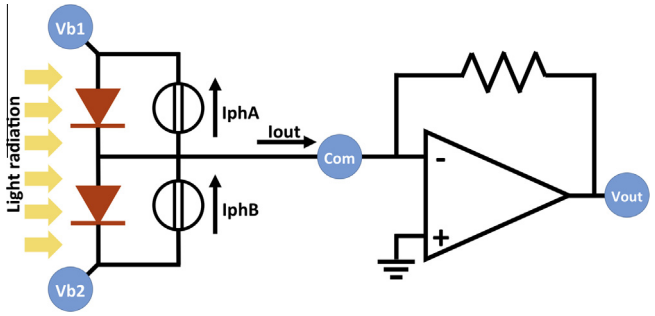

Fig. 2. Electronic circuit corresponding to the balanced photodiode connected through the common electrode to the read-out electronics. The generators in parallel with the diodes represent the induced photocurrents. The transimpedance circuit amplifies only the difference between the diode currents.

electrical connection of the structure to metal pads located on the edge area of the glass substrate.

The fabrication of the whole balanced device requires the use of standard microelectronic technologies: Physical and Chemical Vapour Deposition (PVD and CVD) of thin film, Dry and Wet etching of different materials, photolithographic steps for the geometry patterning.

Four lithographic masks, reported in Fig. 3, have been utilized. In particular, a top-down approach has been used. It consists in the deposition of the whole structure of the device (metal bottom electrode/amorphous silicon junction/metal top electrode), followed by the patterning of the bottom electrodes and of the diode area. This procedure ensures the decrease of defects at the interfaces, which may occur if the thin film is deposited after the photolithography process.

The whole fabrication process included the following steps:

1. Ultrasonic cleaning of the glass substrate;
2. Vacuum evaporation of Cr/Al/Cr 30/200/30 nm three layer metal stack;
3. Plasma Enhanced CVD of heterojunction: a-Si n-type (30 nm) a-Si intrinsic (500 nm) a-SiC p-type (10 nm); to activate the formation of the CrSi layer with the subsequent deposition of Cr, an ultra thin layer of n-doped a-Si:H has been deposited;
4. Sputtering of Cr (5 nm) for the CrSi formation, and sputtering of titanium/tungsten (100 nm);
5. Patterning of the bottom electrode (Mask 1) by:
   - Ti and Cr wet etching,
   - a-Si:H Plasma etching,
   - Cr/Al/Cr wet etching;
6. Patterning of the single diode area (Mask 2) by:
   - Ti and Cr wet etching,
   - a-Si:H Plasma etching;
7. Deposition by Spin coating of a 5 μm thick SU-8, an epoxy-based negative photoresist, as insulating layer;
8. Opening of the window over the diodes and of the via holes for the electrical connections with the bottom metal lines (Mask 3);
9. Sputtering deposition of a 300 nm titanium/tungsten layer;
10. Patterning (Mask 4) by metal wet etching for: the series connection of the two diodes, the connection to the contact pad area, the metal top grid of the two devices.
11. Deposition by Spin coating of a 5 μm thick SU-8 as passivation layer.

In our fabrication process, the two sensors are deposited during the same PECVD process and the structure is designed as symmetrical as possible. However, spatial nonuniformity in the PECVD

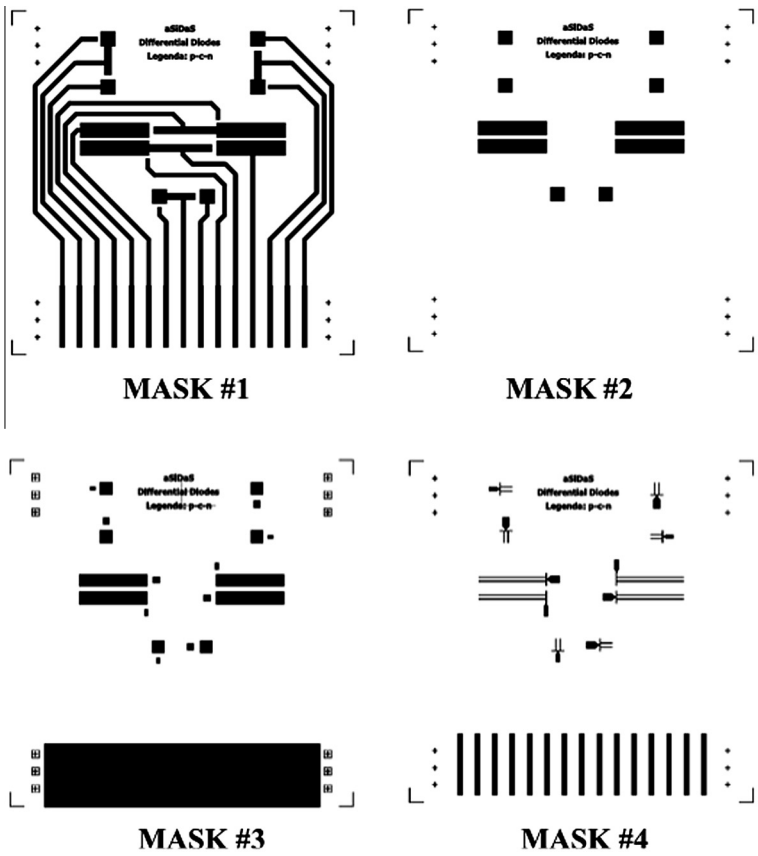

Fig. 3. Photolithographic masks used for the fabrication of the balanced photosensor.

deposition and/or geometrical mismatches can lead to mismatches in the current–voltage characteristics of the two diodes.

The device characterization has been performed by measuring the currents of the two diodes by two Keithley 236 SMU, which provide also the voltage biasing of the structure. The differential current is measured by a Keithley 617 Electrometer, in transimpedance mode, which keeps the output electrode of the balanced structure at ground potential. The measurements have been performed under dark condition and under a 365 nm UV radiation supplied by a standard lamp for biological applications, because the detection of biomolecules in the above mentioned experiments occurred under UV illumination. From data reported in Fig. 4 we found that, in dark condition, the differential current is at least three orders of magnitude lower than the current of each diode and close to the detection limit of our experimental set-up. We also found that, under illumination, the differential signal is about two orders of magnitude lower than the current of each diode.

3.2. Fabrication of the microfluidic channels

Polydimethilsiloxane (PDMS) is widely used silicon-based organic polymer for the fabrication of microfluidic network, and is particularly known for its optical properties and its low manufacturing costs. In our system we have utilized Sylgard 184 from Dow Chemicals that presents excellent transparency characteristics.

Two channels, with dimensions of 3 cm × 2 mm × 150 μm ($L \times W \times H$) for each channel, have been fabricated by pouring of the mixed PDMS on kapton tape mold. After curing at 80 °C for 90 min, the internal surface of the channels has been treated with polyethylene glycol (PEG), also known as polyethylene oxide (PEO), to turn the PDMS hydrophobic properties into hydrophilic properties and thus to allow capillarity flows in the channels.

3.3. Integration of the microfluidic network with the photosensors

At the end of the microfluidic fabrication process, the whole device has been assembled placing the PDMS network over with the balanced photodiode with a gentle pressure and avoiding bubbles between the PDMS and the SU-8 layer.

4. Results and discussion

A picture of the fabricated system is reported in Fig. 5. The PDMS microfluidic network (the rectangular gray shape) lays in the upper right corner of the glass, the differential diode deposited on the glass substrate is highlighted by the red square and the hydrophilic channels are placed horizontally in the figure over the balanced photodiode. In the same figure, the inlets of the two channels are pointed out by the two black arrows, while one outlet hosts a white funnel-shaped bibula paper (highlighted by a red oval) for draining out the solution from the microchannel. The electronic read-out circuit is connected to the three electrodes of the devices by the metal lines at the edge of the substrate.

The experiments have been performed continuously filling the inlets with a pipette in different conditions.

Fig. 6(a) reports the measured currents of the two single diodes and the differential current as function of time under white light. In particular, sensor A is located under channel A, which experiments a filling with water, while sensor B is located under channel B, which remains empty. When water flows in channel A (time between 20 and 100 s), current of sensor A shows an increases of 200 nA over the average value (650 nA). This increase is due to the water that focuses the light over the aligned photosensor. The same 200 nA current increase is measured at the differential

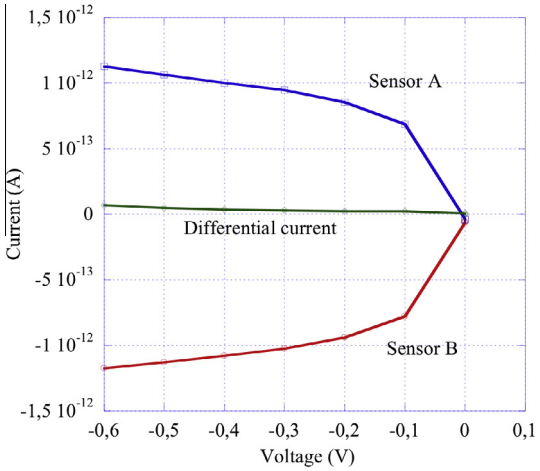

Fig. 4. Current–voltage characteristics in dark conditions and reverse bias voltage of the two n-i-p a-Si:H. The differential current measured at the common electrode of the balanced structure is also shown.

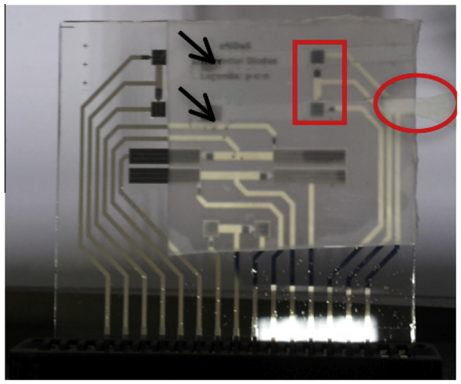

Fig. 5. Picture of the proposed system fabricated on a glass substrate. The hydrophilic channels are placed horizontally in the figure over the balanced photodiode (highlighted by the red square). The two black arrows indicate the inlets of the two channels, while one outlet hosts a white funnel-shaped bibula paper (highlighted by a red oval) for draining out the solution inside the microchannel. (For interpretation of the references to colour in this figure legend, the reader is referred to the web version of this article.)

electrode, which has a background current of 10 nA. When the water stops flowing, currents return to their initial values.

Fig. 6(b) shows the results of a second experiment. In this case, channel A is filled with water in the first 20 s, with a water solution containing fluorescein, in concentration equal to 20 μg/μl, between 20 and 120 s and again with water in the last 80 s. Channel B is continuously filled with water.

A 365 nm UV radiation supplied by a standard lamp for biological applications excites the emission of fluorescence in the fluorescein solution. The three curves in the figure show that, even if the excitation light induces a background current up to about 3.6 μA, the effect of this high value is canceled by the differential measurement. Indeed, in absence of fluorescein the differential current of about 35 nA, very close to the one found in the previous experiment. The presence of fluorescein in the channel induces a photocurrent in the sensor A of about 500 nA, which is the same signal measured at the differential electrode.

These results confirm the effectiveness of our balanced photodetector to reduce of the common mode signals of the background light, and at the same time, to increase the dynamic range of the measurement.

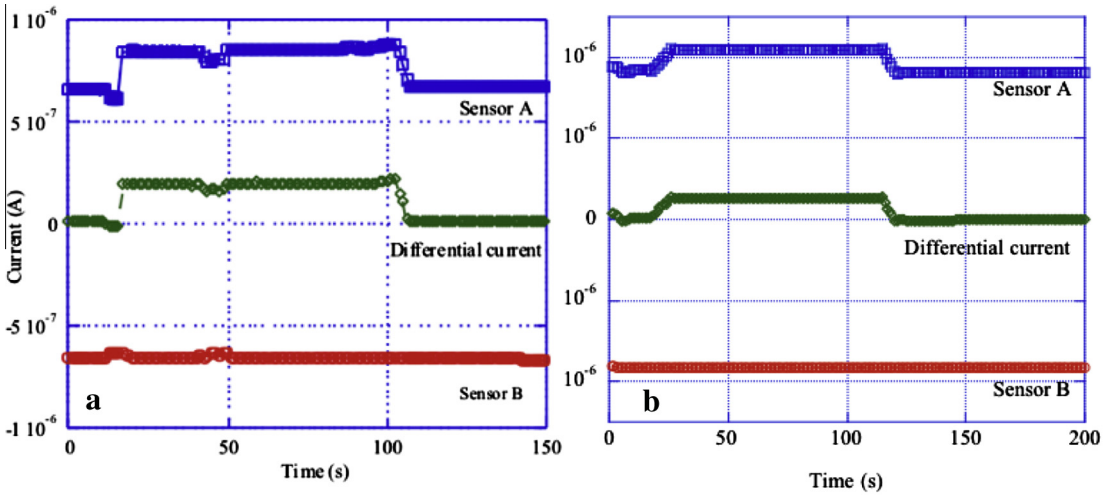

Fig. 6. Differential current and single sensor currents vs time of balanced structure, measured: (a) when water is flowing in channel A in the time interval 20–120 s, and channel B is filled with air, under ambient light; (b) when solution containing fluorescein is flowing in channel A, and water in channel B under UV light.

5. Conclusions

In this paper we focus on the integration of a a-Si:H balanced photodiode integrated with a PDMS hydrophilic two-channel microfluidic network to achieve high-dynamic, high sensitive on-chip detection in a lab-on-chip system. The structure is designed to detect very small differences of light intensities in the two channels in a large background current signal, reducing the common mode signal and increasing the dynamic range of the entire system. The whole device has been deposited on the same side of a glass substrate, optimizing the optical coupling of the differential photosensor with the microfluidic channel and reducing the inter-channel crosstalk.

A fabricated structure demonstrates the ability to reveal the filling with water and the flow of fluorescein inside the channel, rejecting the background light. Future works will be focused on the determination of the limit of detection for different analytes immobilized inside the channels in static and flowing conditions.

Conflict of interest

The authors declared that we have no conflicts of interest to this work.

Acknowledgements

Authors would like to thanks the financial support of the European Community's Seventh Framework Programme FP7-SME-2013 "DEMOTOX " – Proposal No. 604752, the Center for Life Nano Science@Sapienza, Istituto Italiano di Tecnologia (Rome, Italy), the Italian Ministry of Education, University and Research (MIUR) through PRIN2010-2011 project "ARTEMIDE" and the University Project Research 2013 – prot. C26A13HKFB "Lab-on-Chip system for mycotoxin detection in food commodities".

Appendix A. Supplementary data

Supplementary data associated with this article can be found, in the online version, at http://dx.doi.org/10.1016/j.sbsr.2014.12.005.

References

[1] M. Brivio, W. Verboom, D.N. Reinhoudt, Miniaturized continuous flow reaction vessels: influence on chemical reactions, Lab Chip 6 (3) (2006) 329–344.
[2] D. Caputo, G. de Cesare, R. Scipinotti, M. Mirasoli, A. Roda, M. Zangheri, A. Nascetti, Chemiluminescence-based micro-total-analysis system with amorphous silicon photodiodes AISEM 2013, Lect. Notes Electr. Eng. 268 (2014) 207–211.
[3] D. Caputo, G. de Cesare, L.S. Dolci, M. Mirasoli, A. Nascetti, A. Roda, R. Scipinotti, Microfluidic chip with integrated a-Si:H photodiodes for chemiluminescence-based bioassays, IEEE Sens. J. 13 (2013) 2595–2602.
[4] D. Caputo, G. de Cesare, A. Nascetti, R. Negri, R. Scipinotti, Amorphous silicon sensors for single and multicolor detection of biomolecules, IEEE Sens. J. 7 (2007) 1274–1280.
[5] D. Caputo, G. de Cesare, New a-Si: H two terminal switching device for active display, J. Non-Cryst. Solids 198–200 (1996) 1134–1137.
[6] D. Caputo, G. de Cesare, A. Nascetti, M. Tucci, Detailed study of amorphous silicon ultraviolet sensor with chromium silicide window layer, IEEE Trans. Electron Devices 55 (1) (2008) 452–456.
[7] D. Caputo, G. de Cesare, C. Manetti, A. Nascetti, R. Scipinotti, Smart thin layer chromatography plate, Lab Chip 7 (2007) 978–980.
[8] D. Caputo, G. de Cesare, C. Fanelli, A. Nascetti, A. Ricelli, R. Scipinotti, Amorphous silicon photosensors for detection of Ochratoxin A in wine, IEEE Sens. J. 12 (8) (2012) 2674–2679.
[9] D. Caputo, G. de Cesare, A. Nascetti, R. Negri, Spectral tuned amorphous silicon p-i-n for DNA detection, J. Non-Cryst. Solids 352 (2006) 2004–2007.
[10] D. Caputo, G. de Cesare, A. Nascetti, Innovative amorphous silicon balanced ultraviolet photodiode, IEEE Electron Device Lett. 29 (2008) 1299–1301.
[11] D. Caputo, G. de Cesare, A. Nascetti, M. Tucci, Amorphous silicon differential photodiode structure, Sens. Actuators, A 153 (2009) 1–4.
[12] D. Caputo, G. de Cesare, M. Ceccarelli, A. Nascetti, M. Tucci, L. Meda, M. Losurdo, G. Bruno, Characterization of chromium silicide thin layer formed on amorphous silicon films, J. Non-Cryst. Solids 354 (2008) 2171–2175.
[13] D.E. Carlson, C.R. Wronski, Amorphous silicon solar cell, Appl. Phys. Lett. 28 (1976) 671.
[14] F. Costantini, A. Nascetti, R. Scipinotti, F. Domenici, S. Sennato, L. Gazza, F. Bordi, N. Pogna, C. Manetti, D. Caputo, G. de Cesare, On-chip detection of multiple serum antibodies against epitopes of celiac disease by an array of amorphous silicon sensors, RSC Adv. 4 (4) (2014) 2073–2080.
[15] A.G. Crevillen, M. Hervas, M.A. Lopez, M.C. Gonzalez, A. Escarpa, Real sample analysis on microfluidic devices, Talanta 74 (3) (2007) 342–357.
[16] G. de Cesare, M. Gavesi, F. Palma, B. Riccò, A novel a-si: H mechanical stress sensor, Thin Solid Films 427 (1) (2003) 191–195.
[17] G. de Cesare, D. Caputo, A. Nascetti, C. Guiducci, B. Riccò, Hydrogenated amorphous silicon ultraviolet sensor for deoxyribonucleic acid analysis, Appl. Phys. Lett. 88 (2006) 083904-1–083904-3.
[18] L. Erickson, D. Dongqing, Integrated microfluidic devices, Anal. Chim. Acta 507 (2004) 11–26.
[19] D. Eicher, C.A. Merten, Microfluidic devices for diagnostic applications, Expert Rev. Mol. Diagn. 11 (5) (2011) 505–519.
[20] F. Fixe, V. Chu, D. Prazeres, J.P. Conde, An on-chip photodetector for the quantification of DNA probes and targets in microarrays, Nucleic Acids Res. 329 (2004) 70–75.
[21] M.J. Heller, Annu. Rev. Biomed. Eng. 4 (2002) 129.
[22] O. Hofmann, P. Miller, P. Sullivan, T.S. Jones, J.C. de Mello, D.D.C. Bradley, A.J. de Mello, Thin-film organic photodiodes as integrated detectors for microscale chemiluminescence assays, Sens. Actuators B 106 (2005) 878–884.
[23] P. Horowitz, W. Hill, The Art of Electronics, Cambridge University Press, Cambridge, UK, 1989. pp. 98–102.
[24] D.N. Howbrook, A.M. Van der Valk, M.C. O'Shaughnessy, D.K. Sarker, S.C. Baker, A.W. Lloyd, Drug Discov. Today 8 (2003) 642.

[25] D. Janasek, J. Franzke, A. Manz, Scaling and the design of miniaturized chemicalanalysis systems, Nature 442 (7101) (2006) 374–380.
[26] T. Kamei, N.M. Toriello, E.T. Lagally, R.G. Blazej, J.R. Scherer, R.A. Street, R.A. Mathies, Microfluidic genetic analysis with an integrated a-Si:H detector, J. Biomed. Microdevices 7 (2) (2005) 147–152.
[27] T. Kamei, B.M. Paegel, J.R. Scherer, A.M. Skelley, R.A. Street, R.A. Mathies, Integrated hydrogenated amorphous Si photodiode detector for microfluidic bioanalytical devices, Anal. Chem. 75 (2003) 5300–5305.
[28] T.M.H. Lee, M.C. Carles, I.M. Hsing, Microfabricated pcr-electrochemical device for simultaneous DNA amplification and detection, Lab Chip 3 (2) (2003) 100–105.
[29] L. Luan, R.D. Evans, N.M. Jokerst, R.B. Fair, Integrated optical sensor in a digital microfluidic platform, IEEE Sens. J. 8 (2008) 628–635.
[30] L. Malic, D. Brassard, T. Veres, M. Tabrizian, 2010 Integration and detection of biochemical assays in digital microfluidic LOC devices, Lab Chip 10 (2010) 418–431.
[31] F. Mugele, J.C. Baret, Electrowetting: from basics to applications, J. Phys. Condens. Matter 17 (28) (2005) 705.
[32] L. Sandeau, C. Vuillaume, S. Contié, E. Grinenval, F. Belloni, H. Rigneault, R.M. Owens, M. Brennan Fournet, Large area CMOS bio-pixel array for compact high sensitive multiplex biosensing, Lab Chip, 2015, Advance Article Dec 2014, http://dx.doi.org/10.1039/C4LC01025F, Paper First published online: 04.
[33] H. Schaefer, K. Seibel, M. Walder, L. Schoeler, T. Pletzer, M. Waidelich, H. Ihmels, D. Ehrhardt, M. Boehm, Monolithic integrated optical detection for microfluidic systems using thin film photodiodes based on amorphous silicon, in: Proc. 18th IEEE Int. Conf. MEMS, Miami, FL, 2005, p. 758.
[34] R.A. Street, Hydrogenated Amorphous Silicon, Cambridge University Press, New York, 1991.
[35] L.Y. Yeo, H.-C. Chang, P.P. Chan, J.R. Friend, Microuidic devices for bioapplications, Small 7 (1) (2011) 12–48.